JOURNAL OF APPLIED ELECTROCHEMISTRY **27** (1997) 1385–1389

Electrodeposition of Pb–Cu alloy coatings from gluconate baths

S. S. ABD EL REHIM

Chemistry Department Faculty of Science, Ain Shams University, Cairo, Egypt

N. F. MOHAMED, N. H. AMIN, L. I. ALI

Faculty of Education, Ain Shams University, Cairo, Egypt

Received 18 July 1997; revised 2 January 1997

Pb–Cu alloy coatings were electrodeposited on steel sheet cathodes from baths containing mixtures of lead nitrate, copper nitrate and sodium gluconate. Cathodic polarization, cathodic current efficiency and deposit composition were determined under different plating conditions. The results were consistent with the behaviour of a regular plating system with copper being the preferentially depositable metal. The lead (the less noble metal) content in the deposits increased with increase in current density and concentration of lead in the bath but decreased with increase in bath copper concentration. The structure and morphology of the as-deposited coatings were examined by X-ray, AES and SEM. The results showed that the deposits consist of a mixture of fine crystals of the two metals and the morphology of the deposits is mainly controlled by the composition of the deposit.

Keywords: *gluconate baths*, *Pb-Cu alloys*, *steel sheet cathodes*

1. Introduction

The electrodeposition of Pb–Cu alloys has received great attention in order to develop coating for particular purposes, notably wear and corrosion-resistant bearing coatings [1–5].

Pb–Cu alloy coatings have been deposited from both simple and complex ions, typically in acid and alkaline baths respectively [6]. One of the most important baths is a mixed bath containing lead as a tartrate complex and copper as the complex cyanide [7, 8]. Although lead is the less noble metal under most conditions, it deposits preferentially, so that the alloy plating system belongs to the anomalous type. The copper content of the alloy decreases with increases in current density and cyanide content of the bath but increases with increases in tartrate content of the bath. Hespenheide *et al.* [9] reported that lead deposits preferentially from baths based on copper cyanide and lead gluconate complex, yielding Pb–Cu alloy superior to those obtained from cyanide tartrate baths for bearing linear applications. On the other hand, Beerwald and Dohler [10], electrodeposited Cu–Pb alloys from the bath containing copper citrate and lead tartrate and Bollenrath [11] showed that in such baths, lead is less noble than copper and deposits less readily, as would normally be expected. Udupa *et al.* [2] electrodeposited such alloy from a nitrate bath containing cetyltrimethylammonium bromide as additive.

In the present paper, we report on the systematic study of the electrodeposition of Pb–Cu alloy coatings from a non cyanide bath containing lead nitrate, copper nitrate and sodium gluconate. In this bath, both Pb(II) and Cu(II) ions are present predominantly as gluconate complex species [12]. We studied the influence of some plating and operating variables on cathodic polarization, cathodic current efficiency, and composition and structure of the as-deposited alloy coatings.

2. Experimental details

Experiments were carried out in solutions containing $Pb(NO_3)_2$, $Cu(NO_3)_2.5H_2O$ and $NaC_6H_{11}O_7$. All solutions were made immediately prior to use in each run from reagent grade chemicals and doubly distilled water. The pH was adjusted using nitric acid or sodium hydroxide and measured by using a Lseibolo Wien pH meter. The experimental setup was described previously [13] and consisted of a Perspex rectangular cell provided with a plane parallel steel sheet cathode and a platinum sheet anode. Each electrode had dimension of 2.5 cm × 3 cm and filled the cross section of the cell. Before each experiment, the cathode was mechanically polished with 600 mesh emery paper, washed with distilled water, rinsed with ethanol and weighed. All experiments were performed at 25 ± 1 °C. The plating duration was 15 min, after which the cathode was withdrawn, washed with distilled water, dried in dessicator and weighed. The chemical composition of the solid deposited coating was determined by EDX-ray spectrometry (CamScan Cambridge Scanning

0021-891X

Company Ltd). Cathodic current efficiency (CCE) was calculated from the deposited weight and the total coulombs passed. The structure of the deposits was examined by X-ray diffraction analysis using X-ray diffractometry (Siemens D 500/501). Surface morphology of the deposits was tested by scanning electron microscopy (CamScan, Cambride Scanning Company Ltd).

Galvanostatic current density–cathodic potential i/E curves were measured in the rectangular cell using a Potentioscan (Potentiostat, Galvanostat Model 273 EG&G). Potentials were measured relative to a saturated calomel electrode (SCE). To avoid contamination the reference electrode was connected to the steel working electrode via a bridge provided with a Luggin capillary and filled with the solution under test. The i/E curves were recorded using an X–Y recorder (series 2000 Ominographic).

3. Results and discussion

3.1. *Cathodic polarization curves*

Figure 1 shows the galvanostatic i/E curves for the electrodeposition of Pb, Cu and Pb–Cu alloy from the gluconate baths under similar conditions. It is noteworthy that, in these complex solutions, the equilibrium (static) potential of Cu is more positive than that of Pb indicating that Cu behaves as the nobler metal. The polarization curves for both of the individual metals and alloy deposition are similar. Each curve exhibits a well-defined current plateau that increases with increasing bath metal content (Fig. 2), indicating mass transport control. Based on current efficiency calculation [14], hydrogen evolution occurs even at the lowest current density in all cases. Calculated partial polarization curves for each metal and hydrogen evolution are also given in Fig. 1 (dotted lines). The rate of Cu deposition is seen to be lower than the rate of hydrogen evolution but larger than the rate of Pb deposition at all potentials, as expected since Cu is the more noble metal. Nevertheless, at potentials positive of the onset of rapid hydrogen evolution (point B), Cu and Pb can be codeposited (albeit at low efficiency). The sharp increase in the rate of hydrogen evolution at point B can be attributed to the reduction of water [15]. It is obvious from the individual polarization curves that the rate of water reduction in the Cu bath is higher than in the Pb bath. This can be explained on the basis of the difference in water reduction overpotential on the cathode material, i.e., the surface of the deposit [16]. The strong hydrogen evolution at the point B may also inhibit the diffusion of the metal complexes to the diffusion layer possibly to the concurrent hydrogen chemisorption and bubble formation [15].

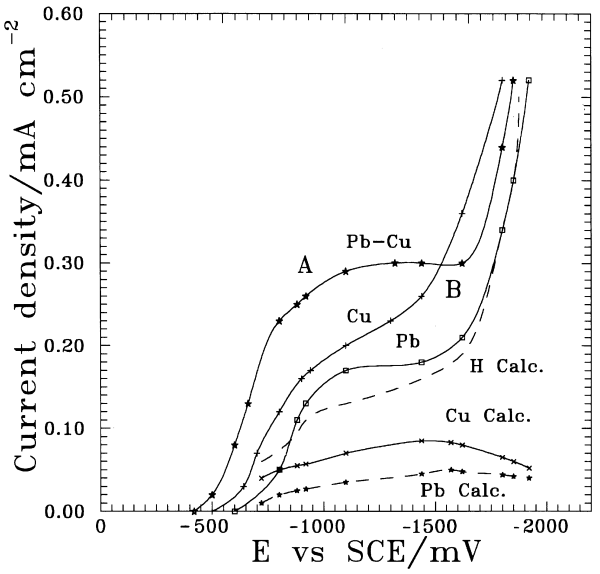

Fig. 1. Experimental (——) polarization curves for Pb from bath containing 21 g dm^{-3} $Pb(NO_3)_2$ and 60 g dm^{-3} sodium gluconate, for Cu from bath containing 18 g dm^{-3} $Cu(NO_3)_2$ $5H_2O$ and 60 g dm^{-3} sodium gluconate and for Pb–Cu alloy from bath containing 21 g dm^{-3} $Pb(NO_3)_2$ + 18 g dm^{-3}$Cu(NO_3)_2.5H_2O$ + 60 g dm^{-3} sodium gluconate at pH 4. (– – –) calculated curves for Pb, Cu and H_2.

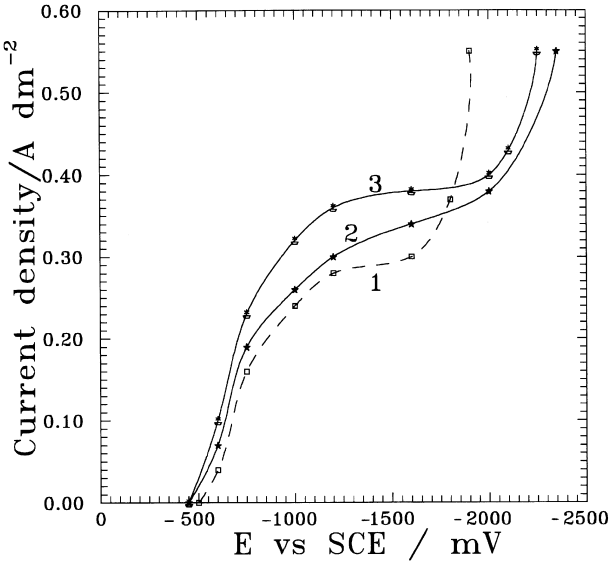

Fig. 2. Cathodic polarization curves for Pb–Cu alloy from baths containing: (a) 21 g dm^{-3} $Pb(NO_3)_2$ + 18 g dm^{-3}$Cu(NO_3)_2.5H_2O$ + 60 g dm^{-3} sodium gluconate. (b) 27 g dm^{-3} $Pb(NO_3)_2$ + 18 g dm^{-3} $Cu(NO_3)_2.5H_2O$ + 60 g dm^{-3} sodium gluconate. (c) 21 g dm^{-3} $Pb(NO_3)_2$ + 24 g dm^{-3} $Cu(NO_3)_2.5H_2O$ + 60 g dm^{-3} sodium gluconate at 25 °C.

3.2. *Composition of the deposits*

Figures 3–7 illustrate the cathodic current efficiency (CCE) and the percentage of lead (Pb) in the deposit as a function of some plating variables. The (CRL) in these figures stands for the composition reference line which is the percentage of Pb in the bath. The data indicate that CCE is less than 100% as a result of simultaneous evolution of hydrogen in all cases studied. The Pb content of the deposits is always below the CRL, indicating normal plating [14] with preferential deposition of Cu (the more noble metal).

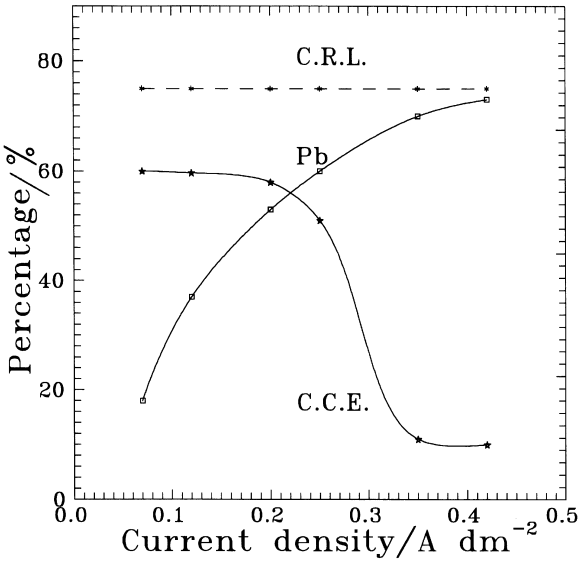

Fig. 3. Effect of current density on CCE and percentage of Pb in the deposit from bath containing 21 g dm^{-3} $Pb(NO_3)_2$ + 18 g dm^{-3} $Cu(NO_3)_2.5H_2O$ + 60 g dm^{-3} sodium gluconate at pH 4. CRL represents the percentage of Pb in the bath.

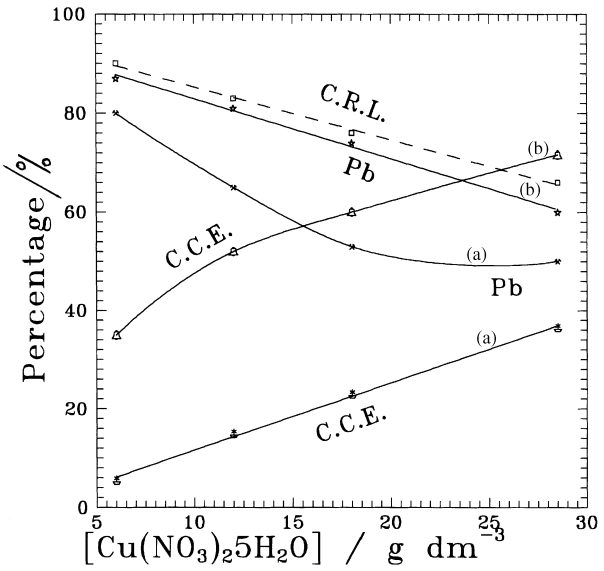

Fig. 5. Effect of $Cu(NO_3)_2.5H_2O$ concentration on CCE and percentage of Pb in the deposits from bath containing 21 g dm^{-3} and 60 g dm^{-3} sodium gluconate. Curves (a) at $i = 0.20$ A dm^{-2} and curves (b) at $i = 0.42$ A dm^{-2}.

Figures 3 and 4 show the current density dependence of CCE and alloy composition. At lower current density (<0.28 A dm^{-2}), the percentage of Pb in the deposit increases gradually with current density. Above this current density which probably corresponds to the limiting current density of alloy deposition, the Pb content of the deposits approximately approaches that of CRL while the CCE drops sharply to about 12% at 0.42 A dm^{-2}. The most likely explanation for these features is that the metal deposition reactions may be suppressed by diffusion inhibiting effect caused by strong magnitude of hydrogen evolution and gas bubbles formation [15]. The fact that the alloy composition at high current densities become identical to the CRL indicates that (under the prevailing conditions) both metal-gluconate complexes have nearly the same values of diffusion coefficient and the thickness of diffusion layer [16].

Figures 4 and 5 show that the percentage of Pb in the deposit increases as the Pb content in the bath increases (at two current densities, 0.20 and 0.42 A dm^{-2}) but decreases with increasing bath Cu content. The CCE increases with increasing metal content of the bath, which minimizes depletion of the metal ions in the diffusion layer.

Figure 6 shows that an increase in the complexing agent (sodium gluconate) concentration has no significant influence on the composition of the deposits but tends to increase the CCE.

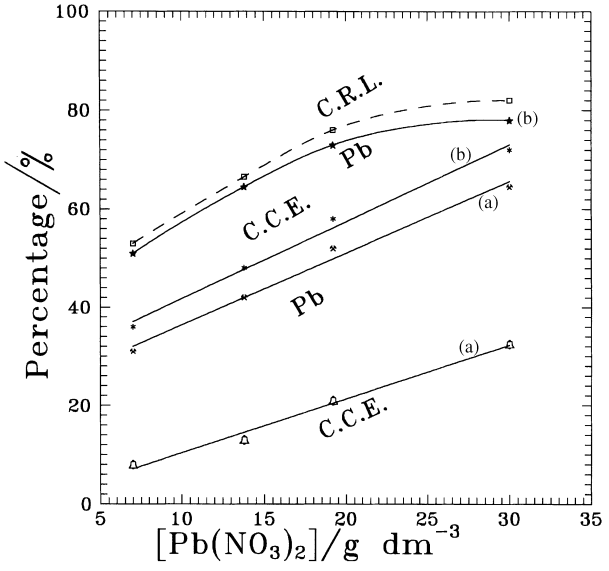

Fig. 4. Effect of $Pb(NO_3)_2$ concentration on CCE and percentage of Pb in the deposits from bath containing 18 g dm^{-3} $Cu(NO_3)_2.5H_2O$ and 60 g dm^{-3} sodium gluconate. Curves (a) at $i = 0.20$ A dm^{-2} and curves (b) at $i = 0.42$ A dm^{-2}.

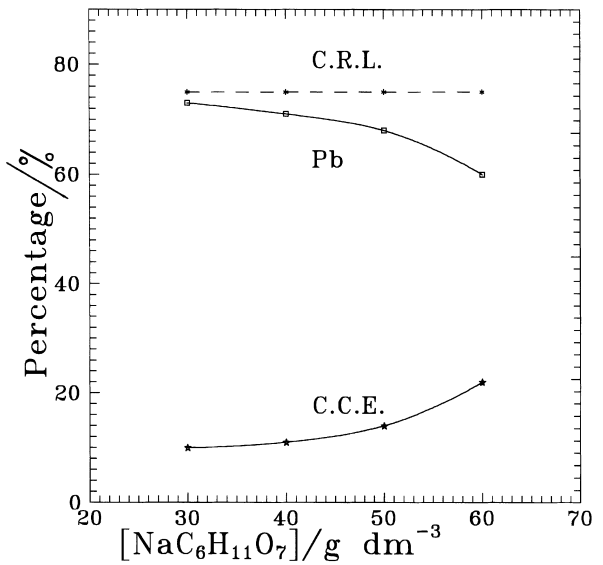

Fig. 6. Effect of sodium gluconate concentration on CCE and percentage of Pb in the deposits from bath containing 21 g dm^{-3} $Pb(NO_3)_2$ + 18 g dm^{-3} $Cu(NO_3)_2.5H_2O$ at $i = 0.42$ A dm^{-2}.

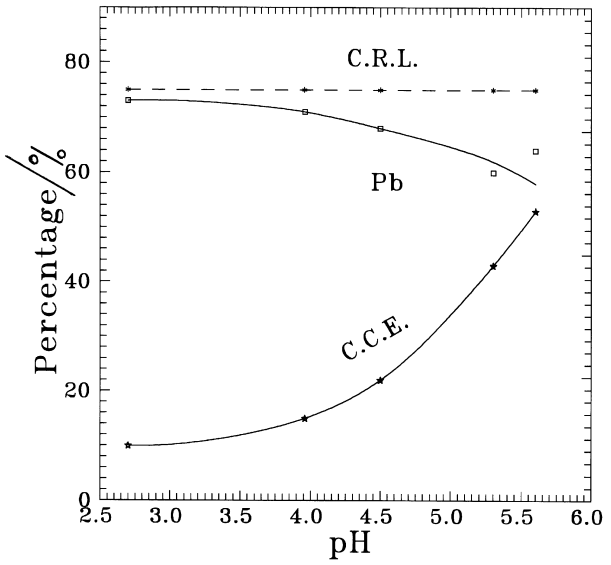

Fig. 7. Effect of bath pH on CCE and percentage of Pb in the deposits from bath containing 21 g dm^{-3} $Pb(NO_3)_2$ + 18 g dm^{-3} $Cu(NO_3)_2.5H_2O$ + 60 g dm^{-3} sodium gluconate at $i = 0.42$ A dm^{-2}.

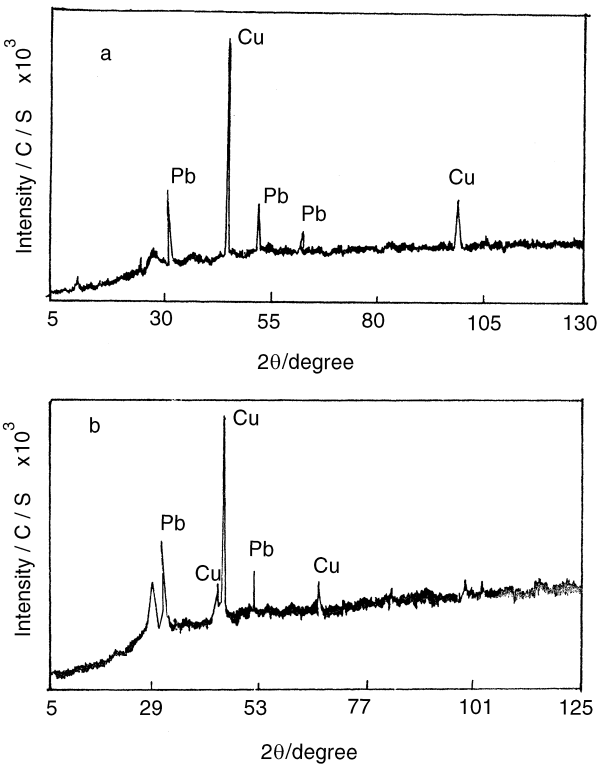

Fig. 8. X-ray diffraction patterns of the as-plated Pb–Cu alloys (a) $i = 0.2$ A dm^{-2}. (b) $i = 0.4$ A dm^{-2}.

Figure 7 reveals that increasing the bath pH decreases (slightly) the percentage of Pb in the deposit and improves the CCE value, possibly because the hydrogen evolution reaction is depressed, or the stabilities of the metal complexes are decreased.

3.3. *Structure and morphology of the deposits*

Compact, semibright and brittle black Pb–Cu deposits were obtained from these baths in most cases. Increasing Pb content of the deposits enhances their smoothness and brightness. Montoro [17] reported that the deposit brittleness is caused by migration and agglomeration of Pb at room temperature, leaving the Cu crystals with no binding material between them. In the present work, X-ray, Auger electron spectroscopy (AES) and scanning electron microscopy (SEM) examinations were carried out on some as-plated coatings obtained from solution containing 21 g dm^{-3} $Pb(NO_3)_2$, 18 g dm^{-3} $Cu(NO_3)_2.5H_2O$ and 60 g dm^{-3} $NaC_6H_{11}O_7$ at pH 4

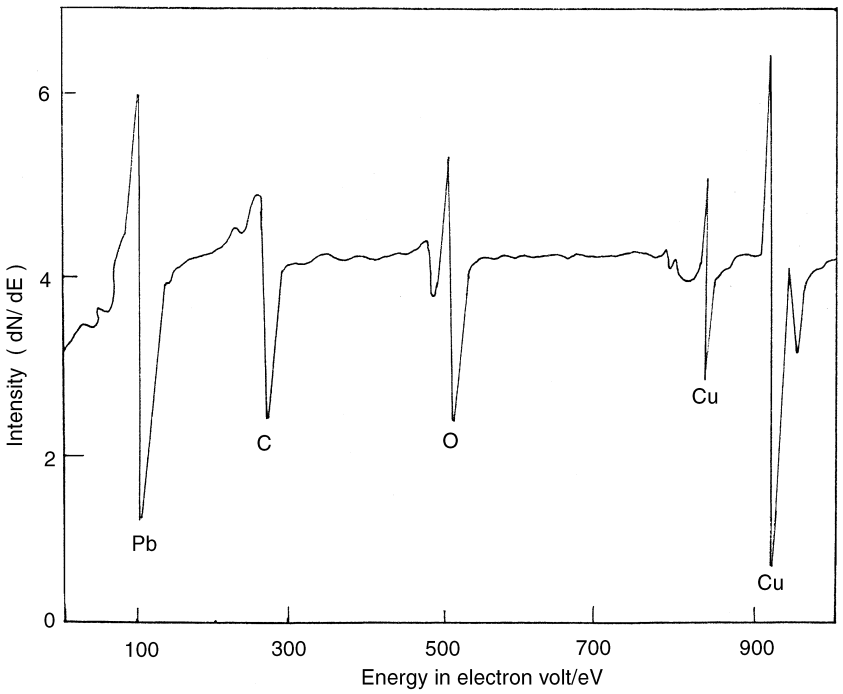

Fig. 9. Auger spectrum of as-deposited Pb–Cu alloy at 0.2 A dm^{-2}.

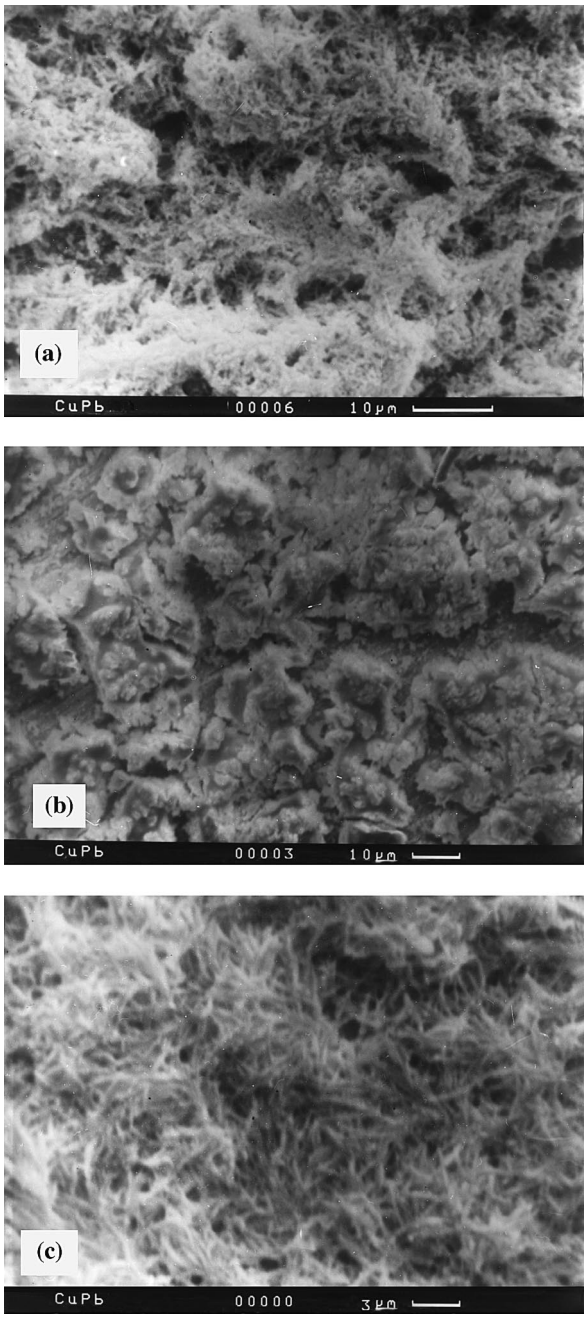

Fig. 10. Photomicrographs of the as-deposited Pb–Cu alloys: (a) $i = 0.07\ \mathrm{A\ dm^{-2}}$, (b) $i = 0.2\ \mathrm{A\ dm^{-2}}$, (c) $i = 0.42\ \mathrm{A\ dm^{-2}}$.

and 25 °C at different current densities. The X-ray diffraction patterns show that the coatings consist of a mixture of crystals of the two metals irrespective of current density used (Fig. 8). These results agree well with those obtained previously whether the deposits were obtained from simple salt bath or from baths containing the metal as complex ions [6]. Agglomeration of the two metals into separate phases is likely because the solubility of Pb in Cu and Cu in Pb is less than 0.01% at room temperature [6]. The Auger spectrum given in Fig. 9 shows all the Auger lines from the deposit constituents, confirming the X-ray diffraction results. The C and O may be attributed to the adsorption of gluconate ions on the surface of the electrode.

Figure 10 shows some representative micrographs of the as-plated coatings. The individual metal grains are apparently too fine to be seen by SEM. However, at low current density ($0.07\ \mathrm{A\ dm^{-2}}$) when the percentage of Pb is low (17%), the deposit is cluster-like, which is characteristic of Cu electrodeposited near the limiting current density (Fig. 10(a)). At higher current density ($0.21\ \mathrm{A\ dm^{-2}}$) when more Pb is codeposited (51%), the deposit becomes smoother (Figure 10(b)). With further increases in the current density ($0.42\ \mathrm{A\ dm^{-2}}$) and Pb content (79%), the hydrogen evolution reaction apparently becomes the dominant process and randomly distributed needle-like grains are observed (Fig. 10(c)). The formation of such dendritic shaped grains probably arises as a consequence of hydrogen gas bubbles clinging to the growth grains [18].

References

[1] E. Raub, *Plat. Surf. Finish.* **63** (1976) 30
[2] H. V. K. Udupa, K. C. Narasimham and P. S. Gomathi, *ibid.* **62** (1975) 1150.
[3] A. A. Qureshi, R. A. Sherwani and Aziz-ur-Rahman, *Pakistan J. Sci. Ind. Res.* **13** (1970) 463.
[4] N. V. Korovin, *Electroplat. Metal Finish.* **17** (1964) 188.
[5] R. A. Schefer, J. F. Cerness and H. A. Thomas, *Trans. Inst. Metal Finish.* **31** (1954) 454.
[6] A. Brenner, 'Electrodeposition of Alloys', Vol. 2, Academic Press, New York (1963).
[7] A. L. Ferguson and N. W. Hovey, *J. Electrochem. Soc.* **98** (1951) 146.
[8] N. W. Hovey, A. K. Rohn and A. L. Ferguson, *ibid.* **98** (1951) 155.
[9] W. G. Hespenheide and C. L. Faust, *US Patent,* 2 739 106 (1956).
[10] A. Beerwald and L. Dohler, *Arch. Metall.* **1** (1947) 412.
[11] F. Bollenrath, *Lufifa hrtforsch* **20** (1943) 284.
[12] A. E. Martell and M. Calvin, 'Chemistry of the Metal Chelate Compounds', Prentice-Hall, Englewood Cliffs, NJ (1956).
[13] S. S. Abd EI Rehim, A. M. Abd EI Halim and M. M. Osman, *J. Chem. Tech. Biotechnol.* **5A** (1985) 415.
[14] A. Brenner 'Electrodeposition of Alloys', Vol. I, Academic Press, New York (1963).
[15] R. Y. Ying and P. K. Ng, *J. Electrochem. Soc.* **135** (1988) 2464.
[16] Y. Fujiwara and H. Enomoto, *Surf. Coat. Technol.* **35** (1988) 101.
[17] V. Montoro, *Met. Finish.* **41** (1949) 279.
[18] E. Raub and A. Engel, *Z. Metallic* **41** (1950) 485.